Spin-Spin interactions in organic magnetoresistance probed by angle-dependent measurements

Spin-Spin Interactions in Organic Magnetoresistance Probed by Angle-Dependent Measurements

W. Wagemans, A. J. Schellekens, M. Kemper, F. L. Bloom, P. A. Bobbert, and B. Koopmans*
Department of Applied Physics, Center for NanoMaterials, Eindhoven University of Technology, P.O. Box 513, 5600 MB Eindhoven, The Netherlands
(Received 5 October 2010; published 10 May 2011)

The dependence of organic magnetoresistance (OMAR) on the orientation of the magnetic field has been investigated. In contrast with previous claims, a finite and systematic change in magnitude is observed when the orientation of the field is changed with respect to the sample. It is demonstrated that, to explain these effects, spin-spin interactions have to be included in the models previously suggested for OMAR. Dipole coupling and exchange coupling are introduced in combination with either an anisotropy of the orientation of the spin pairs or an anisotropy in the hyperfine fields.

DOI: 10.1103/PhysRevLett.106.196802 PACS numbers: 73.43.Qt, 72.80.Le, 75.47.Pq, 85.30.De

In organic devices, considerable changes in the current have been observed when applying a magnetic field [1–9]. The name ''organic magnetoresistance'' (OMAR) has been suggested for this effect [1]. OMAR is generally believed to originate from spin correlations of interacting charge carriers. The spin states of such polaron pairs are mixed by the random hyperfine fields, which can be suppressed by an external magnetic field, resulting in a response on a typical field scale of a few millitesla [2–4]. Gaining a better understanding of the physics of OMAR will improve knowledge of (spin) transport in organic semiconductors and could help realizing possible applications, for instance, in adding magnetic-field sensing to cheap organic electronic devices.

The exact origin of OMAR is still widely debated. Although the spin mechanisms involved are similar, the polarons involved are different in the different models, like the electron-hole (e-h) pair models [2,10–14] and the bipolaron model [3,15]. So far, in the literature it has been claimed that OMAR is independent of the orientation of the applied magnetic field [13,16]. The models suggested for OMAR have not yet included any mechanisms that could give rise to angle dependence.

In this Letter we report on angle-dependent measurements of OMAR. We show that changing the orientation of the applied magnetic field with respect to the sample results in a small but systematic change in the magnitude of OMAR. We show that both anisotropic spin-spin interactions and anisotropic hyperfine fields can explain the observed effects. We conjecture that this may provide a unique tool to discriminate between the suggested models.

We performed experiments on typical OLED-like devices, at room temperature. In discussing our results we will focus on devices with tris-(8-hydroxyquinoline) aluminum (Alq_3) as the active layer. We note that we observed similar results in PPV-based devices. The devices consisted of a glass substrate with a patterned indium tin oxide electrode on which poly(3,4-ethylenedioxythiophene): poly(styrenesulfonate) (PEDOT:PSS) was spin coated (60 nm). Alq_3 (120 nm) was vapor deposited in a high vacuum system inside a nitrogen filled glove box, after which a top electrode consisting of LiF(1 nm)/Al(100 nm) was vapor deposited. The devices (active area 3 mm $\times$ 3 mm) were transported to a different glove box in which they were electrically characterized. By using a dc magnetic field with a small ac modulation, the magnetic-field dependence of the current $I(B)$ could be accurately determined by integrating dI/dB [17]. From $I(B)$, the magnetoconductance was calculated with $\mathrm{MC}(B) = [I(B) - I(0)]/I(0)$. The sample could be rotated with respect to the magnetic field, with an angle θ defined with respect to the sample normal. Both MC(B) at different θ, and $I(\theta)$ at different B were measured.

A small but clear difference in MC was observed between parallel ($\theta = 0°$) and perpendicular ($\theta = 90°$) alignment, with a larger MC for the perpendicular than for the parallel case, see Fig. 1(a). The MC for intermediate angles shows an oscillation as a function of θ, see Fig. 1(b). (A correction was made for a slowly increasing signal due to conditioning [18].) Vertically plotted is MC_∞, which was obtained from fitting the MC(B) curves with a typical ''non-Lorentzian'' that is commonly seen in OMAR measurements: $\mathrm{MC}(B) = \mathrm{MC}_\infty B^2/(|B| + B_0)^2$, where MC_∞ is the MC at infinite magnetic field and B_0 is the half width at quarter maximum [1]. Within the accuracy of the fits, no change in B_0 was found, see Fig. 1(d). The data can be accurately fitted with a $\cos^2\theta$ dependence. Direct measurements of $I(\theta)$ at fixed B confirm these findings (not shown). Moreover, they exclude induction effects from the ac field used. Finally, in Fig. 1(c) we find that the trend in the voltage dependence of the relative change in I, when changing the angle at 250 mT, is identical to the trend in the total magnitude of the MC. In passing, we note that this trend matches the commonly observed [18] MC(V) as shown in the inset of Fig. 1(a). [For the origin of MC(V) many different suggestions have been made [5,13,14,19].] In the plotted voltage range the current changes from

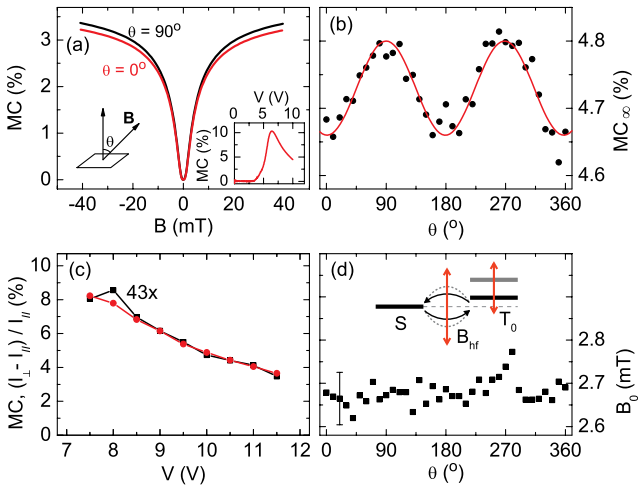

FIG. 1 (color online). (a) MC(B) curves for $\theta = 0°$ and $\theta = 90°$ measured with dI/dB at 12 V with $dB = 0.5$ mT at 27 Hz, with θ as indicated. The inset shows MC(V) at 83 mT [17]. (b), (d) MC_∞ and B_0, obtained from fitting with a non-Lorentzian, as a function of angle. The MC data are fitted with $\cos^2\theta$. (c) MC (circles) and relative change in current (squares, scaled) as a function of voltage at 250 mT. (d) The inset shows energies of S and T_0. The vertical arrows indicate a change in the magnitude of the hyperfine field and in the relative energy difference between S and T_0.

0.3 to 77 A/m^2. From this we conclude that the angle dependence is an intrinsic property of OMAR and not an independent effect.

As the angle dependence appears to be a modulation of the OMAR effect, we have to look at the mechanisms suggested for OMAR to find a possible explanation. In the suggested models, the random hyperfine fields mix spin states of polaron pairs, which either have like charge (bipolarons, e.g., Ref. [3]) or opposite charge (e-h pairs, e.g., Ref. [2]). Such spin pairs can have singlet (S) or triplet (T) character. In the models, at low fields, the hyperfine field mixes S and all T states, while at high field S mixes only with T_0 because T_+ and T_- are Zeeman split with an energy larger than the hyperfine field, resulting in the typical OMAR curves.

Because the angle dependence was found to be largest at large B [Fig. 1(a)], we only have to focus on the mixing between S and T_0. The strength of this mixing is determined by the energy difference between S and T_0 as compared to the hyperfine field $B_{\rm hf}$, see Fig. 1(d). One of these two has to change in magnitude on changing the angle in order to explain the observed angle dependence, as illustrated by the vertical arrows. An energy difference between S and T_0 can originate from spin-spin interactions in the pairs, like exchange coupling or dipole coupling. It will be shown that the observed angle dependence can be explained by a finite spin-spin interaction in combination with an anisotropy in either the hyperfine fields or in the dipole coupling. Besides spin-spin interactions, we excluded several other possible sources of the angle

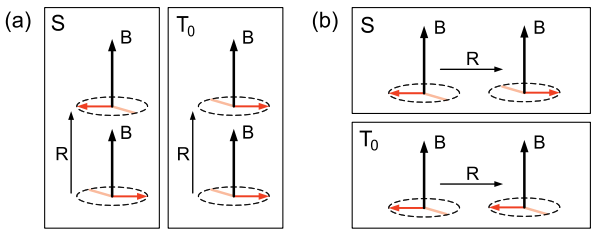

FIG. 2 (color online). Spin pair, in S and T_0 configuration, precessing in a magnetic field **B**, with **B** and the displacement vector **R** either (a) parallel or (b) perpendicular. One third of a full rotation is indicated by the shaded arrows.

dependence [1,20]. We stress that although spin-spin interactions have been qualitatively linked to OMAR in general [2,6,19], they have never been related to a possible angle dependence.

To explain the influence of dipole coupling, first we will discuss it in a simplified way based on a semiclassical picture. We can imagine the two spins of S to be pointing in opposite directions, while they are pointing in the same direction in T_0, see Fig. 2. The dipole energy of two spins pointing in the same direction is larger when they are head to tail than when they are next to each other. This means that for S and T_0 the angle between the magnetic field and the displacement vector **R** (as defined in Fig. 2) affects the strength of the dipole coupling between the two spins. The dipole coupling remains constant on precession of the spin in the magnetic field for **B** and **R** parallel [Fig. 2(a)], while it varies in the perpendicular case [Fig. 2(b)].

To quantitatively study the angle dependence including spin-spin interactions for the different models, it is necessary to use a density matrix description of the spin system of the two interacting polarons. In this treatment, the model can be generalized to cover both the e-h pair models and the bipolaron model [21]. Starting from free carriers, polaron pairs (e-e, h-h, or e-h, depending on the model) are created with a rate r, consisting of $\frac{1}{4}r$ singlets and $\frac{3}{4}r$ triplets. These S and T states can be mixed by the local hyperfine fields. The number of polaron pairs can be reduced via a spin independent step with rate q (e.g., dissociating back into free carriers), and via a spin dependent step with rates k_T and k_S (e.g., bipolaron or exciton formation). Only when k_T and k_S are different the suppression of the mixing by an external field can change the current through the system. This difference is the key assumption of the different models (e.g., $k_T = 0$ for the bipolaron model and $k_T \neq k_S$ for the e-h pair model). In the different models, the resulting MC(B) depends linearly on $\Delta P(B) = P(B) - P(0)$, where $P(B)$ is the probability to perform a spin dependent step.

To calculate P we need to solve the density matrix $\boldsymbol{\rho}$ from its equation of motion, for which we use the stochastic Liouville equation [22,23]:

$$\frac{\partial \boldsymbol{\rho}}{\partial t} = -\frac{i}{\hbar}[\mathbf{H}(t), \boldsymbol{\rho}(t)] - \frac{1}{2}\{\boldsymbol{\Lambda}, \boldsymbol{\rho}(t)\} + \boldsymbol{\Gamma} = 0. \quad (1)$$

The first term is the Liouville term describing the evolution of the density matrix under the influence of the Hamiltonian of the system $\mathbf{H}$; here, the square brackets denote the commutator. This Hamiltonian includes hyperfine interactions, $\mathbf{H}_{\rm hf} = g\mu_B[\mathbf{B}_{\rm hf,1}\cdot\mathbf{S}_1 + \mathbf{B}_{\rm hf,2}\cdot\mathbf{S}_2]$, where μ_B is the Bohr magneton and g is the g factor of a polaron, and Zeeman splitting of the triplets, $\mathbf{H}_Z = g\mu_B\mathbf{B}\cdot(\mathbf{S}_1 + \mathbf{S}_2)$. The second term is a "sink" term that spin-selectively removes particles from the system, using the projection operator $\mathbf{\Lambda}$; here, the curly brackets denote the anticommutator. $\mathbf{\Lambda}$ includes the rate q and projects with prefactor k_T and k_S on the triplet and singlet spin subspace, respectively. The last term $\mathbf{\Gamma}$ is a source term that adds random spin pair states. We investigate the slow hopping regime; i.e., the precession of the spins is much faster than the time between hops. We note that a similar angle dependence can be found in the intermediate hopping regime [20]. For a given configuration, $\boldsymbol{\rho}$ can be solved from Eq. (1). The singlet (ρ_S) and triplet-pair density (ρ_T) are extracted from $\boldsymbol{\rho}$ and used to calculate $P = (k_S\rho_S + k_T\rho_T)/[(k_S + q)\rho_S + (k_T + q)\rho_T]$.

To investigate the effects of spin-spin interactions, dipole coupling and exchange coupling are added. The dipole coupling term that is added to the Hamiltonian is [24] $\mathbf{H}_{\rm dip} = D[\mathbf{S}_1\cdot\mathbf{S}_2 - 3(\mathbf{S}_1\cdot\mathbf{R}/R)(\mathbf{S}_2\cdot\mathbf{R}/R)]$, where $\mathbf{S}_1$ and $\mathbf{S}_2$ are the spin operators of the two spins, and D is the dipole coupling strength; $D = \mu_0 g^2\mu_B^2/(4\pi\hbar R^3)$, where μ_0 is the permeability of free space and $\hbar$ is Planck's constant. For a typical displacement of 1.5 nm, the dipole interaction strength is approximately 1 mT [24]. We note that this is a point dipole approximation, ignoring the three dimensional structure of the molecular orbitals. The exchange term that is added to the Hamiltonian is $\mathbf{H}_{\rm ex} = -J(\frac{1}{2} + 2\mathbf{S}_1\cdot\mathbf{S}_2)$, with J the strength of the interaction. At large fields, where only S-T_0 mixing is relevant due to Zeeman splitting, the absolute energy difference between S and T_0 is $\frac{1}{2}|D(1 - 3\cos^2\alpha) - 4J|$, where α is the angle between the applied field and the displacement vector. This yields an angle-dependent mixing between the S and T_0 states and thus a difference in MC at large fields.

Now that we have introduced all ingredients of our Hamiltonian, we discuss $\Delta P(B)$ obtained with Eq. (1) for two cases referred to as "anisotropic $\mathbf{R}$" and "anisotropic $\mathbf{B}_{\rm hf}$." After that we compare with experiments. First, we include spin-spin interactions (anisotropic $\mathbf{R}$), but use an isotropic hyperfine field. Figure 3(a) shows $\Delta P(B)$ for a parallel and perpendicular alignment of $\mathbf{B}$ and $\mathbf{R}$. For this calculation, we averaged over an isotropic distribution of hyperfine fields with standard deviation $B_{\rm hf}$ [25]. The curves show a typical OMAR shape and, most notably, $\alpha = 90°$ shows a larger magnitude, while the width remains nearly unchanged. The most prominent effect of the dipole coupling is to change the magnitude, which is in agreement with the conclusion from the experiments that the width of the MC curves is not affected.

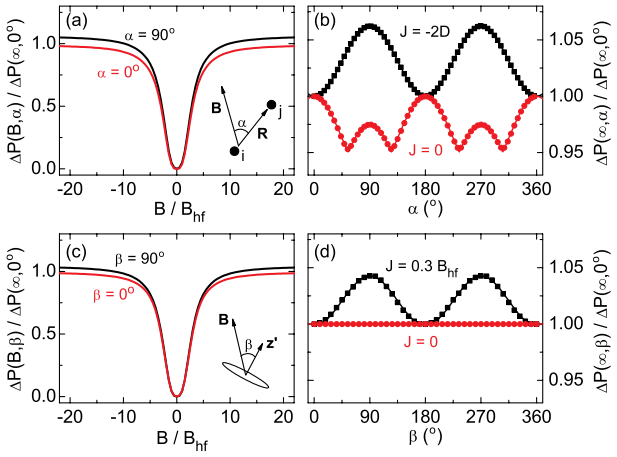

FIG. 3 (color online). Simulated ΔP with (a),(b) anisotropic $\mathbf{R}$ and (c),(d) anisotropic $B_{\rm hf}$, with $q = 1$, $k_S = 1$, and $k_T = 0.1$. (a) P for two orientations of B with $D = 0.03B_{\rm hf}$ and $J = -2D$. (b) Angle dependence with and without exchange coupling. (c) P for two orientations of B with $J = 0.3B_{\rm hf}$ and $B_{{\rm hf},z} = 1.1B_{\rm hf}$. (d) Angle dependence with and without dipole coupling. (b), (d) fitted with $|c_1\cos^2\alpha - c_2|$. The insets schematically represent the angle α between $\mathbf{B}$ and $\mathbf{R}$, and the angle β, between $\mathbf{B}$ and the local axis z'.

In Fig. 3(b), ΔP at infinite magnetic field is plotted as a function of angle. Without exchange coupling ($J = 0$), unlike the experiments, a curve with four maxima is observed. These maxima are caused by the absolute value in the energy difference between S and T_0 being $\frac{1}{2}D|3\cos^2\alpha - 1|$. An angle dependence corresponding with experiments is obtained when also including a small exchange coupling ($J \neq 0$). In OMAR models, the exchange has so far been ignored because, being exponential with distance, it may be expected to either quench the effect or to be negligible. However, in the angle dependence the exchange coupling plays a more important role. If $J \leq -\frac{1}{2}D$, the angle dependence will show a $\cos^2\alpha$ behavior, see Fig. 3(b), otherwise, more maxima are observed. The relative change is largest for $J = -\frac{1}{2}D$. A similar link between exchange and dipole coupling has been suggested before to explain photoluminescence in organic crystals [26].

Next, we investigate the role of an anisotropy of $\mathbf{B}_{\rm hf}$. For this, as an example, we assume an anisotropic region where $\mathbf{B}_{\rm hf}$ is enhanced in the local z' direction with respect to the x' and y' components. Moreover, we average over many random $\mathbf{B}_{\rm hf}$ and assume nonzero isotropic spin-spin interactions by using $J \neq 0$, but note that using an isotropic dipole coupling gives identical results. Also in this case, an angle dependence is found (for the angle β between $\mathbf{B}$ and the z' axis), see Fig. 3(c). We find the largest magnitude for $\mathbf{B}$ perpendicular to the z' axis ($\beta = 90°$). This can also be seen from the P at infinite field as a function of angle in Fig. 3(d). We confirm that no angle dependence is observed when $J = 0$ [Fig. 3(d)], as there is no S-T_0 splitting to probe the anisotropic hyperfine fields, see also Fig. 1(d).

This confirms our conclusion that (isotropic) spin-spin interactions within those pairs that are relevant for OMAR have to be present in our samples.

Now, we will compare the simulated angle dependence of the two different scenarios with the measurements. In the case of anisotropic $\mathbf{R}$, in order to get agreement between the experiments [Figs. 1(a) and 1(b)] and the calculations [Figs. 3(a) and 3(b)], we have to assume $\theta = \alpha$, which corresponds to $\mathbf{R}$ aligning with the sample normal. As was illustrated in Fig. 2, rotating the field with respect to the displacement vector results in a different (average) dipole coupling strength. If we now assume a preferential orientation between the spin pairs in a device, i.e., an anisotropy in the distribution of $\mathbf{R}$, the introduction of a finite dipole coupling will directly give an angle dependence. Such a preferential $\mathbf{R}$ could originate from the electric field enhancing the probability of electrons and holes meeting from opposite directions, or blocking of bipolaron formation on a parallel percolation path.

In the case of anisotropic $\mathbf{B}_{\mathrm{hf}}$ [Figs. 3(c) and 3(d)], we have to assume $\theta = \beta$, which corresponds to the direction of the enhanced hyperfine field aligning with the sample normal. Although the structure of the organic layer is considered to be amorphous, local ordering could give rise to an anisotropy. In the samples, the local breaking of symmetry can either originate from the structure of the sample or from the charge transport. First, it could be the case that the amorphous growth has some anisotropy related to the growth direction, possibly enhanced near the interface. Additionally, even while the number of regions with local order might be small, they might be probed more due to their higher mobility. Second, even without local order, charge transport will select pairs of molecules with favorable mutual alignment. As the charges have to traverse the thickness of the device, the fraction of the hops parallel to the electric field could thus show anisotropy.

Even our basic model with either anisotropic $\mathbf{R}$ or anisotropic $\mathbf{B}_{\mathrm{hf}}$ manages to describe the angle dependence well. It gives, for instance, the correct sign and periodicity, and the effects are of the correct order of magnitude for realistic parameters. So far, we only averaged over the random hyperfine fields, using constant dipole coupling, exchange coupling and transition rates. It is, however, very likely that the values of these parameters are distributed over a certain range, which could lead to subtle changes in the shape of the MC(B) curve [15], its magnitude, and the angle dependence. Moreover, a ''self-selection mechanism'' might be at work where many pairs contribute to the MC, but only some of them have the right combination of parameters to show a noticeable angle dependence.

A challenging task will be to distinguish between the different OMAR models using the angular dependence. We believe this may be possible by performing further experiments with, for instance, magneto-photoluminescence, which could be used to exclude the effects of anisotropy caused by charge transport. Modifying the material such that the average distance between neighboring sites is changed, e.g., by changing side groups of the molecules, could help distinguishing between the role of dipole coupling and exchange coupling and might also result in different effects in the e-h model and the bipolaron model. Another interesting condition for studying angle dependence is around a sign change in MC [5], as it has been suggested to be related to a transition from a bipolaron to an e-h model dominated regime [8], although a small signal to noise ratio might be limiting in this range.

In conclusion, experiments show a clear dependence of the magnitude of OMAR on the orientation of the magnetic field, while the width of the MC(B) curve hardly changes. To explain these effects, spin-spin interactions have to be included in the models. We find that the spin-spin interactions are either anisotropic or are isotropic in combination with anisotropic hyperfine fields. We conjecture that this may provide a unique tool to discriminate between models suggested for OMAR.

This work was supported by the Dutch Technology Foundation (STW) via the NWO VICI-grant ''Spin Engineering in Molecular Devices.''

*b.koopmans@tue.nl

[1] Ö. Mermer *et al.*, Phys. Rev. B **72**, 205202 (2005).
[2] V. N. Prigodin *et al.*, Synth. Met. **156**, 757 (2006).
[3] P. A. Bobbert *et al.*, Phys. Rev. Lett. **99**, 216801 (2007).
[4] P. Desai *et al.*, J. Appl. Phys. **102**, 073710 (2007).
[5] F. L. Bloom *et al.*, Phys. Rev. Lett. **99**, 257201 (2007).
[6] B. Hu and Y. Wu, Nature Mater. **6**, 985 (2007).
[7] U. Niedermeier *et al.*, Appl. Phys. Lett. **92**, 193309 (2008).
[8] F. J. Wang, H. Bassler, and Z. Valy Vardeny, Phys. Rev. Lett. **101**, 236805 (2008).
[9] T. D. Nguyen *et al.*, Nature Mater. **9**, 345 (2010).
[10] E. L. Frankevich *et al.*, Phys. Rev. B **46**, 9320 (1992).
[11] J. Kalinowski *et al.*, Chem. Phys. Lett. **380**, 710 (2003).
[12] Y. Sheng *et al.*, Phys. Rev. B **74**, 045213 (2006).
[13] J. D. Bergeson *et al.*, Phys. Rev. Lett. **100**, 067201 (2008).
[14] S. A. Bagnich *et al.*, J. Appl. Phys. **106**, 113702 (2009).
[15] W. Wagemans *et al.*, J. Appl. Phys. **103**, 07F303 (2008).
[16] T. Francis *et al.*, New J. Phys. **6**, 185 (2004).
[17] W. Wagemans *et al.*, Synth. Met. **160**, 266 (2010).
[18] S. A. Bagnich *et al.*, J. Appl. Phys. **105**, 123706 (2009).
[19] J. Kalinowski, J. Szmytkowski, and W. Stampor, Chem. Phys. Lett. **378**, 380 (2003).
[20] See supplemental material at http://link.aps.org/supplemental/10.1103/PhysRevLett.106.196802 for additional information about the intermediate hopping regime and the g factor.
[21] P. A. Bobbert *et al.*, Synth. Met. **160**, 223 (2010).
[22] R. Johnson and R. Merrifield, Phys. Rev. B **1**, 896 (1970).
[23] A. J. Schellekens *et al.*, Phys. Rev. B (to be published).
[24] A. R. O'Dea *et al.*, J. Phys. Chem. A **109**, 869 (2005).
[25] K. Schulten and P. G. Wolynes, J. Chem. Phys. **68**, 3292 (1978).
[26] R. P. Groff *et al.*, Phys. Rev. B **9**, 2655 (1974).